PHOTONIC SENSORS / Vol. 7, No. 4, 2017: 357–364

Two-Channel Highly Sensitive Sensors Based on 4 × 4 Multimode Interference Couplers

Trung-Thanh LE

International School (VNU-IS), Vietnam National University (VNU), Hanoi, Vietnam

*Corresponding author: Trung-Thanh LE E-mail: thanh.le@vnu.edu.vn

Abstract: We propose a new kind of microring resonators (MRR) based on 4×4 multimode interference (MMI) couplers for multichannel and highly sensitive chemical and biological sensors. The proposed sensor structure has advantages of compactness and high sensitivity compared with the reported sensing structures. By using the transfer matrix method (TMM) and numerical simulations, the designs of the sensor based on silicon waveguides are optimized and demonstrated in detail. We apply our structure to detect glucose and ethanol concentrations simultaneously. A high sensitivity of 9000 nm/RIU, detection limit of 2×10^{-4} for glucose sensing and sensitivity of 6000 nm/RIU, detection limit of 1.3×10^{-5} for ethanol sensing are achieved.

Keywords: Biological sensors; chemical sensors; optical microring resonators; high sensitivity; multimode interference; transfer matrix method; beam propagation method (BPM); multichannel sensor

Citation: Trung-Thanh LE, "Two-Channel Highly Sensitive Sensors Based on 4 × 4 Multimode Interference Couplers," *Photonic Sensors*, 2017, 7(4): 357–364.

1. Introduction

Current approaches to the real-time analysis of chemical and biological sensing applications utilize systematic approaches such as mass spectrometry for detection. Such systems are expensive, heavy, and cannot monolithically integrated in one single chip [1]. Electronic sensors use metallic probes to produce electro-magnetic noise, which can disturb the electro-magnetic field being measured. This can be avoided in the case of using integrated optical sensors. Integrated optical sensors are very attractive due to their advantages of high sensitivity, ultra-wide bandwidth, low detection limit, compactness, and immunity to electromagnetic interference [2, 3].

A large class of optical sensors based on optical fiber and waveguides use the evanescent wave to monitor the presence of the analyte in the environment. Detection can be made by the optical absorption of the analytes, optic spectroscopy or the refractive index change [1]. The two former methods can be directly obtained by measuring optical intensity. The third method is to monitor various chemical and biological systems via the sensing of the change in the refractive index [4]. Optical waveguide devices can perform as refractive index sensors particularly when the analyte becomes a physical part of the device, such as the waveguide cladding. In this case, the evanescent portion of the guided mode within the cladding will overlap and interact with the analyte. The measurement of the refractive index change of the guided mode of the optical waveguides requires a special structure to convert the refractive index change into detectable signals. A number of refractive index sensors based

Received: 6 June 2017 / Revised: 5 July 2017

DOI: 10.1007/s13320-017-0441-1
Article type: Regular

on optical waveguide structures have been reported, including Bragg grating sensors, directional coupler sensors, Mach-Zehnder interferometer (MZI) sensors, microring resonator sensors, and surface plasmon resonance sensors [1, 4–7].

Recently, the use of optical microring resonators as sensors [6] is becoming one of the most attractive candidates for optical sensing applications because of its ultra-compact size and easiness to realize an array of sensors with a large scale integration [8, 9]. When detecting target chemicals by using microring resonator sensors, one can use a certain chemical binding on the surface. There are two ways to measure the presence of the target chemicals. One is to measure the shift of the resonant wavelength, and the other is to measure the optical intensity with a fixed wavelength.

In the literature, some highly sensitive resonator sensors based on polymer and silicon microring and disk resonators have been developed [10, 11]. However, multichannel sensors based on silicon waveguides, which have ultra-small bends due to the high refractive index contrast and are compatible with the existing complementary metal-oxide-semiconductor (CMOS) fabrication technologies, are not presented much. In order to achieve multichannel capability, multiplexed single microring resonators must be used. This leads to a large footprint area and low sensitivity. For example, recent results showed that the sensitivities of 108 nm/RIU [2, 12] and 200 nm/RIU [13] for glucose and ethanol detection using single microring resonator can be achieved. In addition, by using microfluidics with grating, ethanol sensor with a sensitivity of 50 nm/RIU can be obtained [14]. The silicon waveguide based sensors have attracted much attention for realizing ultra-compact and cheap optical sensors. In addition, the reported sensors can be capable of determining only one chemical or biological element.

The sensing structures based on one microring resonator or Mach-Zehnder interferometer can only provide a small sensitivity and single anylate detection [15]. Therefore, in this paper, we present a new structure for achieving a highly sensitive and multichannel sensor. Our structure is based on only one 4 × 4 multimode interference (MMI) coupler assisted microring resonators. The proposed sensors provide a very high sensitivity compared with the conventional MZI sensors. In addition, it can measure two different and independent target chemicals and biological elements simultaneously. We investigate the use of our proposed structure to glucose and ethanol sensing at the same time.

2. Two-channel sensor based on 4× 4 MMI couplers

The proposed sensor based on the 4 × 4 multimode interference and microring resonator structures is shown in Fig. 1. The two MMI couplers are identical. The two 4 × 4 MMI couplers have the same width W_{MMI} and length L_{MMI}.

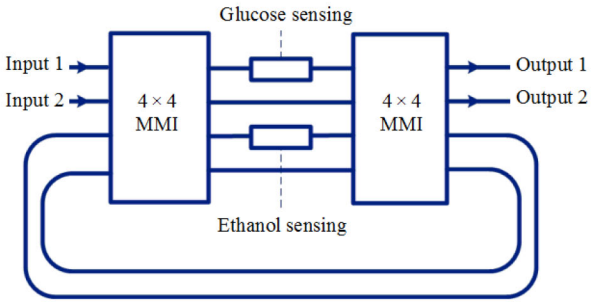

Fig. 1 Schematic of the new sensor using 4 × 4 MMI couplers and microring resonators.

In this structure, there are two sensing windows having lengths L_{arm1} and L_{arm2}. As with the conventional MZI sensor device, segments of two MZI arms overlap with the flow channel, forming two separate sensing regions. The other two MZI arms are isolated from the analyte by the micro fluidic substrate. The MMI coupler consists of a multimode optical waveguide that can support a number of modes [16]. In order to launch and extract light from the multimode region, a number of single mode access waveguides are placed at the input and output planes. If there are N input waveguides and M output waveguides, then the

device is called an $N\times M$ MMI coupler.

The operation of the optical MMI coupler is based on the self-imaging principle [16, 17]. Self-imaging is a property of a multimode waveguide by which the input field is reproduced in single or multiple images at periodic intervals along the propagation direction of the waveguide. The central structure of the MMI filter is formed by a waveguide designed to support a large number of modes.

In this study, the access waveguides are identical single mode waveguides with width W_a. The input and output waveguides are located as follows[18]:

$$x_i = \left(i+\frac{1}{2}\right)\frac{W_{\mathrm{MMI}}}{N}, \quad i=0,\ 1,\ \cdots,\ N-1. \tag{1}$$

The electrical field inside the MMI coupler can be expressed as follows [19]:

$$E(x,z)=\exp(-\mathrm{j}kz)\sum_{m=1}^{M}E_m\exp\left(\mathrm{j}\frac{m^2\pi}{4\Lambda}z\right)\sin\left(\frac{m\pi}{W_{\mathrm{MMI}}}x\right). \tag{2}$$

In this study, the length of the MMI coupler is to be $L_{\mathrm{MMI}}=\frac{3L_\pi}{2}$, where L_π is the beat length of the MMI coupler. One can prove that the normalized optical powers transmitting through the proposed sensor at the wavelengths on resonance with the microring resonators are given as [9, 20]

$$T_1=\left\{\frac{\alpha_1-\left|\cos\left(\frac{\Delta\varphi_1}{2}\right)\right|}{1-\alpha_1\left|\cos\left(\frac{\Delta\varphi_1}{2}\right)\right|}\right\}^2 \tag{3}$$

$$T_2=\left\{\frac{\alpha_2-\left|\cos\left(\frac{\Delta\varphi_2}{2}\right)\right|}{1-\alpha_2\left|\cos\left(\frac{\Delta\varphi_2}{2}\right)\right|}\right\}^2 \tag{4}$$

where $\tau_1=\sin\left(\frac{\Delta\varphi_1}{2}\right)$, $\kappa_1=\cos\left(\frac{\Delta\varphi_1}{2}\right)$, $\tau_2=\sin\left(\frac{\Delta\varphi_2}{2}\right)$, and $\kappa_2=\cos\left(\frac{\Delta\varphi_2}{2}\right)$; $\Delta\varphi_1$ and $\Delta\varphi_2$ are the phase differences between two arms of the MZI, respectively; α_1 and α_2 are round trip transmissions of light propagation through the two microring resonators [21].

In this study, the locations of the input and output waveguides, and MMI width and length are carefully designed, so the desired characteristics of the MMI coupler can be achieved. It is now shown that the proposed sensor can be realized by using the silicon nanowire waveguides [22, 23]. By using the numerical method, the optimal width of the MMI is calculated to be $W_{\mathrm{MMI}}=6\mu\mathrm{m}$ for the high performance and compact device. The core thickness is $h_{\mathrm{co}}=220\,\mathrm{nm}$. The access waveguide is tapered from a width of 500 nm to a width of 800 nm to improve the device performance. It is assumed that the designs are for the transverse electric (TE) polarization at a central optical wavelength $\lambda=1550\mathrm{nm}$. The finite difference time domain (FDTD) simulations for sensing operation when the input signal is at Ports 1 and 2 for glucose and ethanol sensing are shown in Figs. 2(a) and 2(b), respectively. The mask design for the whole sensor structure by using the CMOS technology is shown in Fig. 2(c).

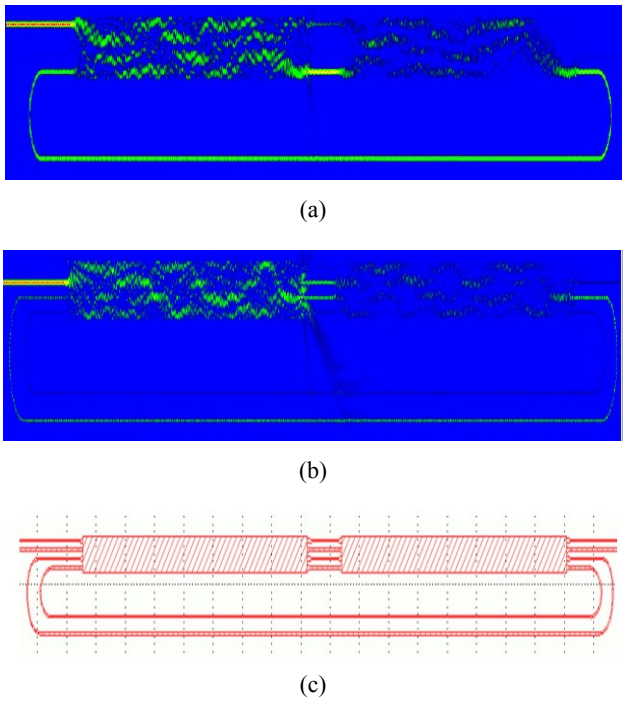

(a) (b) (c)

Fig. 2 FDTD simulations for two-channel sensors: (a) glucose, (b) ethanol, and (c) mask design.

The proposed structure can be viewed as a

sensor with two-channel sensing windows, which are separated with two power transmission characteristics T_1 and T_2, and sensitivities S_1 and S_2. When the analyte is presented, the resonance wavelengths are shifted. As the result, the proposed sensors are able to monitor two target chemicals simultaneously, and their sensitivities can be expressed as

$$S_1 = \frac{\partial \lambda_1}{\partial n_c} \quad \text{and} \quad S_2 = \frac{\partial \lambda_2}{\partial n_c} \tag{5}$$

where λ_1 and λ_2 are resonance wavelengths of the transmissions at Outputs 1 and 2, respectively.

For the conventional sensor based on the MZI structure, the relative phase shift $\Delta\varphi$ between two MZI arms and the optical power transmitting through the MZI can be made a function of the environmental refractive index, via the modal effective index n_{eff}. The transmission at the bar port of the MZI structure can be given as [1]

$$T_{\text{MZI}} = \cos^2\left(\frac{\Delta\varphi}{2}\right) \tag{6}$$

where $\Delta\varphi = 2\pi L_{\text{arm}}(n_{\text{eff},a} - n_{\text{eff},0})/\lambda$, L_{arm} is the interaction length of the MZI arm, $n_{\text{eff},a}$ is the effective refractive index in the interaction arm when the ambient analyte is presented, and $n_{\text{eff},0}$ is the effective refractive index of the reference arm. From (3), (5), and (6), the ratio of the sensitivities of the proposed sensor and the conventional MZI sensor can be numerically evaluated. The sensitivity enhancement factor S_1 / S_{MZI} can be calculated for values of α_1 between 0 and 1, which is plotted in Fig. 3. For $\alpha_1 = 0.99$, an enhancement factor of approximately 10 is obtained. The similar results can be achieved for other sensing arms.

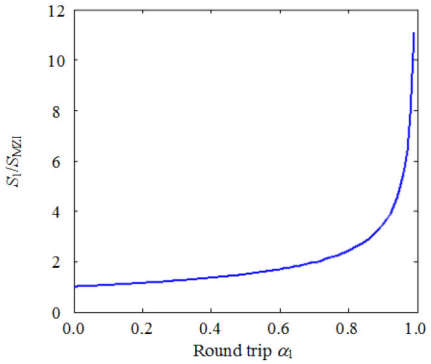

Fig. 3 Sensitivity enhancement factor for the proposed sensor, calculated with the first sensing arm.

3. Results and discussion

In general, our proposed structure can be used for the detection of chemical and biological elements by using both surface and homogeneous mechanisms. Without the loss of generality, we apply our structure to the detection of glucose and ethanol sensing as an example. The refractive indexes of the glucose (n_{glucose}) and ethanol (n_{ethanol}) can be calculated from the concentration (C%) based on the experimental results at wavelength 1550 nm as [24, 25]

$$n_{\text{glucose}} = 0.2015x[C] + 1.3292 \tag{7}$$

$$n_{\text{ethanol}} = 1.3292 + a[C] + b[C]^2 \tag{8}$$

where $a = 8.4535 \times 10^{-4}$ and $b = -(4.8294 \times 10^{-6})$. The refractive indexes of the glucose and ethanol at different concentrations are shown in Fig. 4. In our design, the silicon waveguide with a height of 220 nm and a width of 500 nm is used for single mode operation. The wavelength is 1550 nm. It is assumed that the interaction length for glucose and ethanol sensing arms is 100μm. By using the finite difference method (FDM), the effective refractive indexes of the waveguide at different concentrations are shown in Fig. 5.

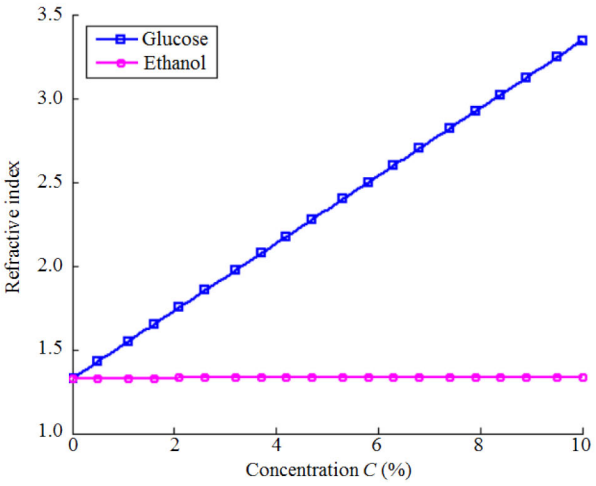

Fig. 4 Refractive indexes of the glucose and ethanol verus concentations.

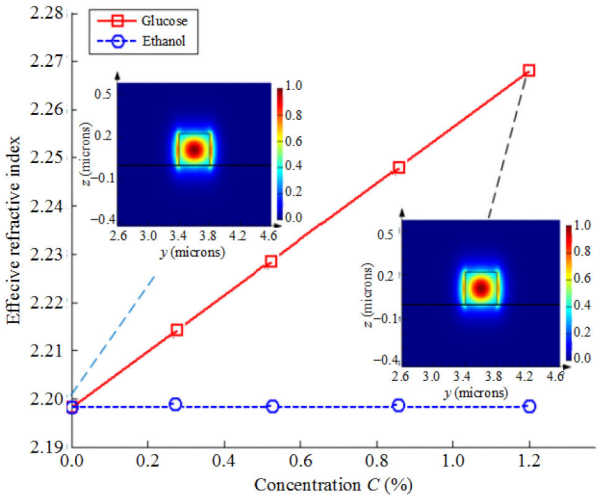

Fig. 5 Effective refractive indexes of the waveguide with glucose and ethanol covers at different concentrations.

The glucose solutions with concentrations of 0%, 0.2%, and 0.4% and ethanol concentrations of 0%, 3%, and 6% are induced to the device. The resonance wavelength shifts corresponding to the concentrations can be measured by the optical spectrometer as shown in Fig. 6 for glucose and Fig. 7 for ethanol. For each 0.2% increment of the glucose concentration, the resonance wavelength shift of about 10^5 pm is achieved. This is a greatly higher order than that of the recent conventional sensor based on the single microring resonator [25, 26]. For each 3% increment of the ethanol concentration, the resonance wavelength shift of about 1.5×10^4 pm is achieved.

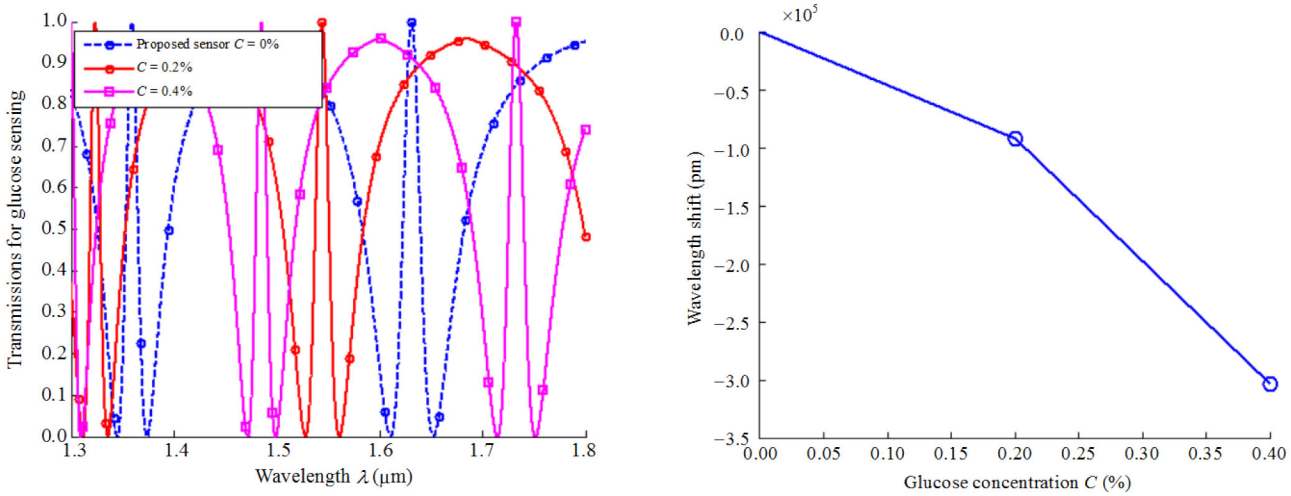

(a) (b)

Fig. 6 Characteristics of the glucose sensor: (a) transmissions at the output port 1 for glucose sensing and (b) resonance wavelength shift at different glucose concentrations.

By measuring the resonance wavelength shift ($\Delta\lambda$), the glucose concentration is detected. The sensitivity of the glucose sensor can be calculated as follows:

$$S_{\text{glucose}} = \frac{\Delta\lambda}{\Delta n} = 9000(\text{nm/ RIU}) . \quad (9)$$

Our sensor provides the sensitivity of 9000 nm/RIU compared with a sensitivity of 170 nm/RIU [26].

In addition to the sensitivity, the detection limit (DL) is another important parameter. For the refractive index sensing, the DL presents for the smallest ambient refractive index change, which can be accurately measured. The DL can be calculated as the ratio of the resonance wavelength resolution σ to the sensitivity S_{glucose} by [27]

$$DL = \frac{\sigma}{S_{\text{glucose}}} \quad (10)$$

where $\sigma = \sqrt{\sigma^2_{\text{amp-noise}} + \sigma^2_{\text{temp-induced}} + \sigma^2_{\text{spec-res}}}$, $\sigma_{\text{amp-noise}}$ is the standard deviation of the spectral variation which is determined by the Q factor and extinction ratio, $\sigma_{\text{temp-induced}}$ is the standard deviation induced by noises in the sensing systems, and

$\sigma_{\text{spec-res}}$ is resulted from the spectral resolution of the optical spectrometer. In our sensor design, we use the optical refractometer with a resolution of 20 pm, the detection limit of our sensor is calculated to be 2×10^{-4}, compared with a detection limit of 1.78×10^{-5} of the single microring resonator sensor [28].

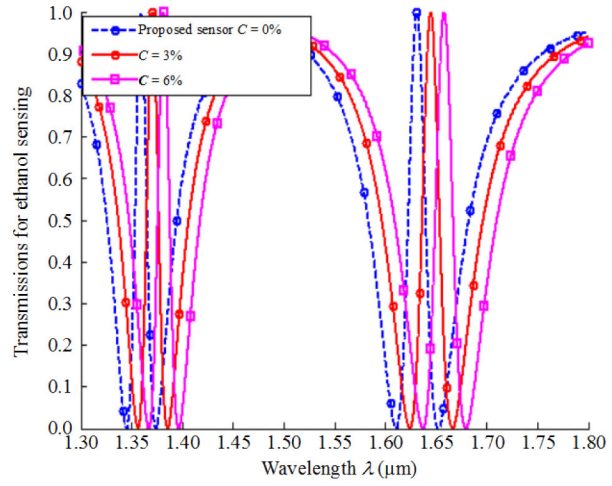

(a)

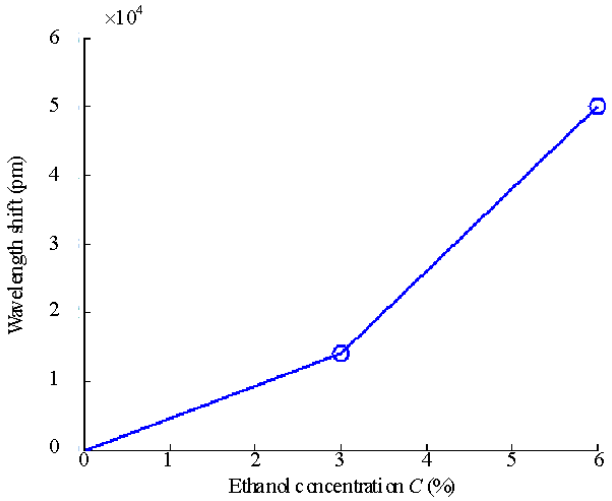

(b)

Fig. 7 Characteristics of ethanol sensor: (a) transmissions at the output port 2 for ethanol sensing and (b) resonance wavelength shift at different ethanol concentrations.

The sensitivity of the ethanol sensor is calculated to be $S_{\text{ethanol}} = 6000\,\text{nm/RIU}$, and the detection limit is 1.3×10^{-5}.

Silicon waveguides are highly sensitive to temperature fluctuations due to the high thermo-optic coefficient (TOC) of silicon ($\text{TOC}_{\text{Si}} = 1.86\times10^{-4}\,\text{K}^{-1}$). As a result, the sensing performance will be affected due to the phase drift. In order to overcome the effect of the temperature and phase fluctuations, we can use some approaches including both active and passive methods. For example, the local heating of silicon itself to dynamically compensate for any temperature fluctuations [29], material cladding with negative thermo-optic coefficient [30–33], MZI cascading intensity interrogation [34], control of the thermal drift by tailoring the degree of optical confinement in silicon waveguides with different waveguide widths [35], and ultra-thin silicon waveguides [36] can be used for reducing the thermal drift.

4. Conclusions

We have presented a novel sensor structure based on the 4×4 multimode interference structure and microring resonators. The design of the proposed sensors uses silicon waveguides, therefore, the sensor has advantages of compatibility with the CMOS fabrication technology and compactness. It has been shown that the proposed sensors can provide a very high sensitivity of 9000 nm/RIU for glucose solution and 6000 nm/RIU for ethanol solution compared with the conventional sensors. In addition, by using the 4×4 multimode interference couplers, our sensor structure can detect glucose and ethanol solutions simultaneously.

Acknowledgment

This research is funded by Vietnam National University, Hanoi (VNU) under project number QG.15.30.

References

[1] V. M. N. Passaro, F. Dell'Olio, B. Casamassima, and F. D. Leonardis, "Guided-wave optical biosensors," *Sensors*, 2007, 7(4): 508–536.

[2] C. Ciminelli, C. M. Campanella, F. Dell'Olio, C. E. Campanella, and M. N. Armenise, "Label-free optical resonant sensors for biochemical applications," *Progress in Quantum Electronics*, 2013, 37(2): 51–107.

[3] W. Wang, *Advances in chemical sensors*. Rijeka, Croatia: InTech, 2012: 1–346.

[4] L. Shi, Y. H. Xu, W. Tan, and X. F. Chen, "Simulation of optical microfiber loop resonators for ambient refractive index sensing," *Sensors*, 2007, 7(5): 689–696.

[5] H. X. Yi, D. S. Citrin, and Z. P. Zhou, "Highly sensitive silicon microring sensor with sharp asymmetrical resonance," *Optics Express*, 2010, 18(13): 2967–2972.

[6] Z. X. Xia, Y. Chen, and Z. P. Zhou, "Dual waveguide coupled microring resonator sensor based on intensity detection," *IEEE Journal of Quantum Electronics*, 2008, 44(1–2): 100–107.

[7] V. M. N. Passaro, F. Dell'Olio, and F. De Leonardis, "Ammonia optical sensing by microring resonators," *Sensors*, 2007, 7(11): 2741–2749.

[8] C. Le. Arce, K. De Vos, T. Claes, K. Komorowska, D. Van Thourhout, and P. Bienstman, "Silicon-on-insulator microring resonator sensor integrated on an optical fiber facet," *IEEE Photonics Technology Letters*, 2011, 23(13): 890–892.

[9] T. T. Le, "Realization of a multichannel chemical and biological sensor using 6 × 6 multimode interference structures," *International Journal of Information and Electronics Engineering,* Singapore, 2011, 2: 240–244.

[10] K. De Vos, J. Girones, T. Claes, Y. De Koninck, S. Popelka, E. Schacht, *et al.*, "Multiplexed antibody detection with an array of silicon-on-insulator microring resonators," *IEEE Photonics Journal*, 2009, 1(4): 225–235.

[11] D. X. Dai, "Highly sensitive digital optical sensor based on cascaded high-*Q* ring-resonators," *Optics Express*, 2009, 17(26): 23817–23822.

[12] Y. Chen, Z. Y. Li, H. X. Yi, Z. P. Zhou, and J. Yu, "Microring resonator for glucose sensing applications," *Frontiers of Optoelectronics in China*, 2009, 2(3): 304–307.

[13] G. D. Kim, G. S. Son, H. S. Lee, K. D. Kim, and S. S. Lee, "Integrated photonic glucose biosensor using a vertically coupled microring resonator in polymers," *Optics Communications*, 2008, 281(18): 4644–4647.

[14] C. Errando-Herranz, F. Saharil, A. M. Romero, N. Sandstrom, R. Z. Shafagh, W. Van Der Wijingaart, *et al.*, "Integration of microfluidics with grating coupled silicon photonic sensors by one-step combined photopatterning and molding of OSTE," *Optics Express*, 2013, 21(18): 21293–21298.

[15] A. F. Gavela, D. G. García, J. C. Ramirez, and L. M. Lechuga, "Last advances in silicon-based optical biosensors," *Sensors*, 2016, 16(3): 1–15.

[16] L. B. Soldano and E. C. M. Pennings, "Optical multi-mode interference devices based on self-imaging: principles and applications," *Journal of Lightwave Technology*, 1995, 13(4): 615–627.

[17] M. Bachmann, P. A. Besse, and H. Melchior, "General self-imaging properties in $N \times N$ multimode interference couplers including phase relations," *Applied Optics*, 1994, 33(18): 3905–3911.

[18] T. T. Le, *Multimode interference structures for photonic signal processing*. Saarbrücken, Germany: LAP LAMBERT Academic Publishing, 2010: 1–328.

[19] J. M. Heaton and R. M. Jenkins, "General matrix theory of self-imaging in multimode interference (MMI) couplers," *IEEE Photonics Technology Letters*, 1999, 11(2): 212–214.

[20] T. T. Le and L. Cahill, "Generation of two Fano resonances using 4 × 4 multimode interference structures on silicon waveguides," *Optics Communications*, 2013, 301–302: 100–105.

[21] W. M. J. Green, R. K. Lee, G. DeRose, A. Scherer, and A. Yariv, "Hybrid InGaAsP-InP Mach-Zehnder racetrack resonator for thermooptic switching and coupling control," *Optics Express*, 2005, 13(5): 1651–1659.

[22] T. T. Le and L. W. Cahill, "The design of 4 × 4 multimode interference coupler based microring resonators on an SOI platform," *Journal of Telecommunications and Information Technology*, 2009: 98–102.

[23] D. T. Le, M. C. Nguyen, and T. T. Le, "Fast and slow light enhancement using cascaded microring resonators with the Sagnac reflector," *Optik*, 2017, 131: 292–301.

[24] X. P. Liang, Q. Z. Zhang, and H. B. Jiang, "Quantitative reconstruction of refractive index distribution and imaging of glucose concentration by using diffusing light," *Applied Optics*, 2006, 45(32): 8360–8365.

[25] C. Ciminelli, F. Dell'Olio, D. Conteduca, C. M. Campanella, and M. N. Armenise, "High performance SOI microring resonator for biochemical sensing," *Optics & Laser Technology*, 2014, 59: 60–67.

[26] O. A. Marsh, Y. L. Xiong, and W. N. Ye, "Slot waveguide ring-assisted Mach-Zehnder interferometer for sensing applications," *IEEE Journal of Selected Topics in Quantum Electronics*, 2017, 23(2): 440–443.

[27] J. J. Hu, X. C. Sun, A. Agarwal, and L. C. Kimerling, "Design guidelines for optical resonator biochemical sensors," *Journal of the Optical Society of America*

B-Optical Physics, 2009, 26(5): 1032–1041.
[28] Y. Chen, Y. L. Ding, and Z. Y. Li, "Ethanol Sensor Based on Microring Resonator," *Advanced Materials Research*, 2013: 655–657.
[29] S. Manipatruni, R. K. Dokania, B. Schmidt, N. Sherwood Droz, C. B. Poitras, A. B. Apsel, *et al.*, "Wide temperature range operation of micrometer-scale silicon electro-optic modulators," *Optics Letters*, 2008, 33(19): 2185–2187.
[30] M. Han and A. Wang, "Temperature compensation of optical microresonators using a surface layer with negative thermo-optic coefficient," *Optics Letters*, 2007, 32(13): 1800–1802.
[31] K. B. Gylfason, A. M. Romero, and H. Sohlström, "Reducing the temperature sensitivity of SOI waveguide-based biosensors," *SPIE*, 2012: 84310F–1–84310F–15.
[32] C. T. Wang, C. Y. Wang, J. H. Yu, I. T. Kou, C. W. Tseng, H. C. Jau, *et al.*, "Highly sensitive optical temperature sensor based on a SiN micro-ring resonator with liquid crystal cladding," *Optics Express*, 2016, 24(2): 1002–1007.
[33] F. Qiu, F. Yu, A. M. Spring, and S. Yokoyama, "Athermal silicon nitride ring resonator by photobleaching of disperse red 1-doped poly(methyl methacrylate) polymer," *Optics Letters*, 2012, 37(19): 4086–4088.
[34] X. Y. Han, Y. C. Shao, X. N. Han, Z. L. Lu, Z. L. Wu, J. Teng, *et al.*, "Athermal optical waveguide microring biosensor with intensity interrogation," *Optics Communications*, 2015, 356: 41–48.
[35] B. Guha, B. B. C. Kyotoku, and M. Lipson, "CMOS-compatible athermal silicon microring resonators," *Optics Express*, 2010, 18(4): 3487–3493.
[36] S. T. Fard, V. Donzella, S. A. Schmidt, J. Flueckiger, S. M. Grist, P. Talebi Fard, *et al.*, "Performance of ultra-thin SOI-based resonators for sensing applications," *Optics Express*, 2014, 22(12): 14166–14179.